

Double Quantization for Communication-Efficient Distributed Optimization

Yue Yu¹, Jiaxiang Wu², Longbo Huang¹

¹Institute for Interdisciplinary Information Sciences, Tsinghua University

²Tencent AI Lab

yu-y14@mails.tsinghua.edu.cn, jonathanwu@tencent.com, longbohuang@tsinghua.edu.cn

Abstract

Modern distributed training of machine learning models suffers from high communication overhead for synchronizing stochastic gradients and model parameters. In this paper, to reduce the communication complexity, we propose *double quantization*, a general scheme for quantizing both model parameters and gradients. Three communication-efficient algorithms are proposed under this general scheme. Specifically, (i) we propose a low-precision algorithm AsyLPG with asynchronous parallelism, (ii) we explore integrating gradient sparsification with double quantization and develop Sparse-AsyLPG, (iii) we show that double quantization can also be accelerated by momentum technique and design accelerated AsyLPG. We establish rigorous performance guarantees for the algorithms, and conduct experiments on a multi-server test-bed to demonstrate that our algorithms can effectively save transmitted bits without performance degradation.

1 Introduction

Distributed optimization has received much recent attention due to data explosion and increasing model complexity. The *data parallel* mechanism is a widely used distributed architecture, which decomposes the time consuming gradient computations into sub-tasks, and assigns them to separate worker machines for execution. Specifically, the training data is distributed to M workers and each worker maintains a local copy of model parameters. At each iteration, each worker computes the gradient of a mini-batch randomly drawn from its local data. The global stochastic gradient is then computed by synchronously aggregating M local gradients. Model parameters are then updated accordingly.

Two issues significantly slow down methods based on the data parallel architecture. One is the communication complexity. For example, all workers must send their entire local gradients to the master node at each iteration. If gradients are dense, the master node has to receive and send $M * d$ floating-point numbers per iteration (d is the size of the model vector), which scales linearly with network and model vector size. With the increasing computing cluster size and model complexity, it has been observed in many systems that such communication overhead has become the performance bottleneck [28, 26]. The other factor is the synchronization cost, i.e., the master node has to wait for the last local gradient arrival at each iteration. This coordination dramatically increases system's idle time.

To overcome the first issue, many works focus on reducing the communication complexity of gradients in the data parallel architecture. Generally, there are two kinds of methods. One is quantization [2], which stores gradients using fewer number of bits (lower precision). The other is sparsification [1], i.e., dropping out some coordinates of gradients following certain rules. However, existing communication-efficient algorithms based on data-parallel network still suffer from significant synchronization cost. To address the second issue, many asynchronous algorithms have recently been developed for distributed training [12, 17]. By allowing workers to communicate with master without synchronization, they can effectively improve the training

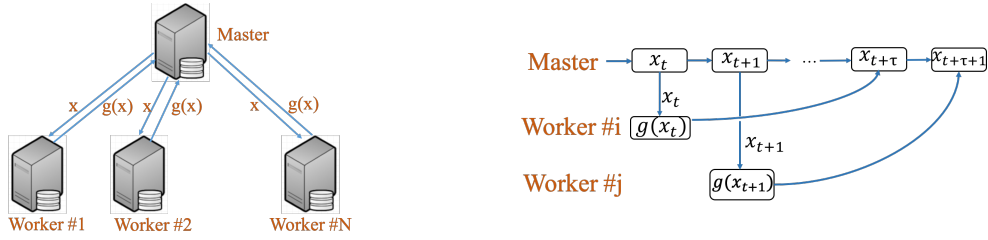


Figure 1: The framework of distributed network with asynchronous communication. Left: network structure. Right: training process.

efficiency. Unfortunately, the communication bottleneck caused by transmitting gradients in floating-point numbers still exists.

In this paper, we are interested in jointly achieving communication-efficiency and asynchronous parallelism. Specifically, we study the following composite problem

$$\min_{x \in \Omega} P(x) = f(x) + h(x), \quad f(x) = \frac{1}{n} \sum_{i=1}^n f_i(x), \quad (1)$$

where $x \in \mathbb{R}^d$ is the model vector, $f_i(x)$ is smooth and $h(x)$ is convex but can be nonsmooth. Domain $\Omega \subseteq \mathbb{R}^d$ is a convex set. This formulation has found applications in many different areas, such as multi-agent optimization [13] and distributed machine learning [8].

To solve (1), we propose a new *double quantization* scheme, which quantizes both model parameters and gradients. This quantization is nontrivial, because we have to deal with a low-precision gradient, which is evaluated on a low-precision model vector. Three communication-efficient algorithms are then proposed under double quantization. We analyze the precision loss of low-precision gradients and prove that these algorithms achieve fast convergence rate while significantly reducing the communication cost. The main contributions are summarized as follows.

(i) We propose an **asynchronous low-precision** algorithm AsyLPG to solve the nonconvex and nonsmooth problem (1). We show that AsyLPG achieves the same asymptotic convergence rate as the unquantized serial algorithm, but with significantly less communication cost.

(ii) We combine gradient sparsification with double quantization and propose Sparse-AsyLPG to further reduce communication overhead. Our analysis shows that the convergence rate scales with $\sqrt{d/\varphi}$ for a sparsity budget φ .

(iii) We propose accelerated AsyLPG, and mathematically prove that double quantization can be accelerated by momentum technique [14, 20].

(iv) We conduct experiments on a multi-server distributed test-bed. The results validate the efficiency of our algorithms.

2 Related Work

Designing large-scale distributed algorithms for machine learning has been receiving an increasing attention, and many algorithms, both synchronous and asynchronous, have been proposed, e.g., [16, 4, 12, 9]. In order to reduce the communication complexity, researches also started to focus on cutting down transmitted bits per iteration, based mainly on two schemes, i.e., quantization and sparsification.

Quantization. Algorithms based on quantization store a floating-point number using limited number of bits. For example, [19] quantized gradients to a representation of $\{-1, 1\}$. [2, 25, 26] adopted an unbiased gradient quantization with multiple levels. The error-feedback method was applied in [19, 26] to integrate history quantization error into the current stage. [7] proposed a low-precision framework of SVRG [10], which quantized model parameters for single machine computation. [28] proposed an end-to-end low-precision scheme, which quantized data, model and gradient with synchronous parallelism. A biased quantization with

gradient clipping was analyzed in [27]. [6] empirically studied asynchronous and low-precision SGD on logistic regression.

Sparsification. Methods on sparsification drop out certain coordinates of gradients. [1] only transmitted gradients exceeding a threshold. [24, 22] formulated gradient sparsification into an optimization problem to balance sparsity and variance. Recently, [21, 3] analyzed the convergence behavior of sparsified SGD with memory, i.e., compensating gradient with sparsification error.

Our work distinguishes itself from the above results in: (i) We quantize both model vectors and gradients. (ii) We integrate gradient sparsification within double quantization and prove the convergence. (iii) We analyze how double quantization can be accelerated to reduce communication rounds.

Notation. x^* is the optimal solution of (1). $\|x\|_\infty$, $\|x\|_1$ and $\|x\|$ denote the max, L_1 and L_2 norm of x . For a vector $v_t \in \mathbb{R}^d$, $[v_t]_i$ or $v_{t,i}$ denotes its i -th coordinate. $\{e_i\}_{i=1}^d$ is the standard basis in \mathbb{R}^d . The base of logarithmic function is 2. $\tilde{O}(f)$ denotes $O(f \cdot \text{polylog}(f))$. We use the proximal operator to handle the nonsmooth $h(x)$, i.e., $\text{prox}_{\eta h}(x) = \arg \min_y h(y) + \frac{1}{2\eta} \|y - x\|^2$. If problem (1) is nonconvex and nonsmooth, we apply the commonly used convergence metric *gradient mapping* [15]: $G_\eta(x) \triangleq \frac{1}{\eta} [x - \text{prox}_{\eta h}(x - \eta \nabla f(x))]$. x is defined as an ϵ -accurate solution if it satisfies $\mathbf{E} \|G_\eta(x)\|^2 \leq \epsilon$.

3 Preliminary

3.1 Low-Precision Representation via Quantization

Low-precision representation stores numbers using limited number of bits, contrast to the 32-bit full-precision.¹ It can be represented by a tuple (δ, b) , where $\delta \in \mathbb{R}$ is the scaling factor and $b \in \mathbb{N}^+$ is the number of bits used. Specifically, given a tuple (δ, b) , the set of representable numbers is

$$\text{dom}(\delta, b) = \{-2^{b-1} \cdot \delta, \dots, -\delta, 0, \delta, \dots, (2^{b-1} - 1) \cdot \delta\}.$$

For any full-precision $x \in \mathbb{R}$, we call the procedure of transforming it to a low-precision representation as quantization, which is denoted by function $Q_{(\delta, b)}(x)$. It outputs a number in $\text{dom}(\delta, b)$ according to the following rules:

(i) If x lies in the convex hull of $\text{dom}(\delta, b)$, i.e., there exists a point $z \in \text{dom}(\delta, b)$ such that $x \in [z, z + \delta]$, then x will be stochastically rounded in an unbiased way:

$$Q_{(\delta, b)}(x) = \begin{cases} z + \delta, & \text{with probability } \frac{x-z}{\delta}, \\ z, & \text{with probability } \frac{z+\delta-x}{\delta}. \end{cases}$$

(ii) Otherwise, $Q_{(\delta, b)}(x)$ outputs the closest point to x in $\text{dom}(\delta, b)$, i.e., the minimum or maximum value.

This quantization method is widely used in existing works, e.g., [28, 2, 25, 7], sometimes under different formulation. In the following sections, we adopt $Q_{(\delta, b)}(v)$ to denote quantization on vector $v \in \mathbb{R}^d$, which means that each coordinate of v is independently quantized using the same tuple (δ, b) . Low-precision representation can effectively reduce communication cost, because we only need $(32 + bd)$ bits to transmit quantized $Q_{(\delta, b)}(v)$ (32 bits for δ , and b bits for each coordinate), whereas it needs $32d$ bits for a full-precision v .

3.2 Distributed Network with Asynchronous Communication

As shown in Figure 1, we consider a network with one master and multiple workers, e.g., the parameter-server setting. The master maintains and updates a model vector x , and keeps a training clock. Each worker gets

¹We assume without loss of generality that a floating-point number is stored using 32 bits (also see [2, 27]). Our results can extend to the case when numbers are stored with other precision.

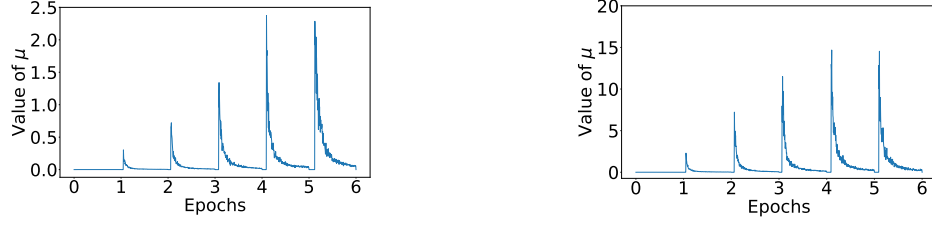


Figure 2: The value of μ in different epochs that guarantees (2). Left: $b_x = 8$. Right: $b_x = 4$. The statistics are based on a logistic regression on dataset *covtype* [5].

access to the full datasets and keeps a disjoint partition of data. In each communication round, a worker retrieves x from the master, evaluates the gradient $g(x)$, and then sends it back to the master. Since workers asynchronously pull and push data during the training process, at a time t , the master may use a delayed gradient calculated on a previous $x_{D(t)}$, where $D(t) \leq t$. Many works showed that a near linear speedup can be achieved if the delay is reasonably moderate [12, 17].

4 Algorithms

To solve problem (1), we propose a communication-efficient algorithm with double quantization, namely AsyLPG, and introduce its two variants with gradient sparsification and momentum acceleration. We begin with the assumptions made in this paper. They are mild and are often assumed in the literature, e.g., [10, 18].

Assumption 1. *The stochastically sampled gradient is unbiased, i.e., for $a \in \{1, \dots, n\}$ sampled in Step 11 of Algorithms 1, 2, 3, $\mathbf{E}_a[\nabla f_a(x)] = \nabla f(x)$. Moreover, the random variables in different iterations are independent.*

Assumption 2. *Each $f_i(x)$ in (1) is L -Lipschitz smooth, i.e., $\|\nabla f_i(x) - \nabla f_i(y)\| \leq L\|x - y\|$, $\forall x, y \in \Omega$.*

Assumption 3. *The gradient delay is upper bounded by some finite constant $\tau > 0$, i.e., $t - D(t) \leq \tau$, $\forall t$.*

4.1 Communication-Efficient Algorithm with Double Quantization: AsyLPG

In this section, we introduce our new distributed algorithm AsyLPG, with **asynchronous** communication and **low-precision** floating-point representation. As shown in Algorithm 1, AsyLPG divides the training procedure into epochs, similar to SVRG [10], with each epoch containing m inner iterations. At the beginning of each epoch, AsyLPG performs one round of communication between the master and workers to calculate the full-batch gradient $\nabla f(\tilde{x}^s)$, where \tilde{x}^s is a snapshot variable evaluated at the end of each epoch s . This one round communication involves full-precision operation because it is only performed once per epoch, and its communication overhead is small compared to the subsequent m communication rounds in inner iterations, where the model parameters are updated.

In inner iterations, the communication between the master and workers utilizes the asynchronous parallelism described in Section 3.2. To reduce communication complexity, we propose *double quantization*, i.e., quantizing both model parameters and gradients.

Model Parameter Quantization. In Step 8, before transmitting $x_{D(t)}^{s+1}$, the master quantizes it into a low-precision format, subject to the following constraint:

$$\mathbf{E}_Q \|Q_{(\delta_x, b_x)}(x_{D(t)}^{s+1}) - x_{D(t)}^{s+1}\|^2 \leq \mu \|x_{D(t)}^{s+1} - \tilde{x}^s\|^2. \quad (2)$$

This condition is set to control the precision loss of $x_{D(t)}^{s+1}$ with a positive hyperparameter μ . Note that with a larger μ , we can aggressively save more transmitted bits (using a smaller b_x). In practice, the precision

Algorithm 1 AsyLPG

```
1: Input:  $S, m, \eta, b_x, b, \tilde{x}^0 = x^0$ ;  
2: for  $s = 0, 1, \dots, S - 1$  do  
3:    $x_0^{s+1} = \tilde{x}^s$ ;  
4:   /* Map-reduce global gradient computation */  
5:   Compute  $\nabla f(\tilde{x}^s) = \frac{1}{n} \sum_{i=1}^n \nabla f_i(\tilde{x}^s)$ ;  
6:   for  $t = 0$  to  $m - 1$  do  
7:     /* For master: */  
8:     (i) Model Parameter Quantization: Set  $\delta_x = \frac{\|x_{D(t)}^{s+1}\|_\infty}{2^{b-1}-1}$  and quantize  $x_{D(t)}^{s+1}$  subject to (2). Then,  
       send  $Q_{(\delta_x, b_x)}(x_{D(t)}^{s+1})$  to workers;  
9:     (ii) Receive local gradient  $Q_{(\delta_{\alpha_t}, b)}(\alpha_t)$ ,  
       compute  $u_t^{s+1} = Q_{(\delta_{\alpha_t}, b)}(\alpha_t) + \nabla f(\tilde{x}^s)$ , and  
       update  $x_{t+1}^{s+1} = \text{prox}_{\eta h}(x_t^{s+1} - \eta u_t^{s+1})$ ;  
10:    /* For worker: */  
11:    (i) Receive  $Q_{(\delta_x, b_x)}(x_{D(t)}^{s+1})$ , stochastically sample a data-point  $a \in \{1, \dots, n\}$ , and calculate gradient  $\alpha_t = \nabla f_a(Q_{(\delta_x, b_x)}(x_{D(t)}^{s+1})) - \nabla f_a(\tilde{x}^s)$ ;  
12:    (ii) Gradient Quantization: Set  $\delta_{\alpha_t} = \frac{\|\alpha_t\|_\infty}{2^{b-1}-1}$  and send the quantized gradient  $Q_{(\delta_{\alpha_t}, b)}(\alpha_t)$  to the master;  
13:  end for  
14:   $\tilde{x}^{s+1} = x_m^{s+1}$ ;  
15: end for  
16: Output: Uniformly choosing from  $\{\{x_t^{s+1}\}_{t=0}^{m-1}\}_{s=0}^{S-1}$ .
```

loss and communication cost can be balanced by selecting a proper μ . On the other hand, from the analysis aspect, we can always find a μ that guarantees (2) throughout the training process, for any given b_x (the number of quantization bits). In the special case when $x_{D(t)}^{s+1} = \tilde{x}^s$, the master only needs to send a flag bit since \tilde{x}^s has already been stored at the workers, and (2) still holds. Figure 2 validates the practicability of (2), where we plot the value of μ required to guarantee (2). Note that the algorithm already converges in both graphs. In this case, we see that when b_x is 4 or 8, μ can be upper bounded by a constant. Also, by setting a larger μ , we can choose a smaller b_x . The reason μ increases at the beginning of each epoch is because $\|x_{D(t)}^{s+1} - \tilde{x}^s\|^2$ is small. After several inner iterations, $x_{D(t)}^{s+1}$ moves further away from \tilde{x}^s . Thus, a smaller μ suffices to guarantee (2).

Gradient Quantization. After receiving the low-precision model parameter, as shown in Steps 11-12, a worker calculates a gradient α_t and quantizes it into its low-precision representation $Q_{(\delta_{\alpha_t}, b)}(\alpha_t)$, and then sends it to the master.

In Step 9, the master constructs a semi-stochastic gradient u_t^{s+1} based on the received low-precision $Q_{(\delta_{\alpha_t}, b)}(\alpha_t)$ and the full-batch gradient $\nabla f(\tilde{x}^s)$, and updates the model vector x using step size η . The semi-stochastic gradient evaluated here adopts the variance reduction method proposed in SVRG [10] and is used to accelerate convergence. If Algorithm 1 is run without *double quantization* and asynchronous parallelism, i.e., only one compute node with no delay, [18] showed that:

Theorem 1. ([18], Theorem 5) Suppose $h(x)$ is convex and Assumptions 1, 2 hold. Let $T = Sm$ and $\eta = \rho/L$ where $\rho \in (0, 1/2)$ and satisfies $4\rho^2 m^2 + \rho \leq 1$. Then for the output x_{out} of Algorithm 1, we have

$$\mathbf{E}\|G_\eta(x_{out})\|^2 \leq \frac{2L(P(x^0) - P(x^*))}{\rho(1 - 2\rho)T}.$$

4.1.1 Theoretical Analysis

We begin with the following lemma which bounds the variance of the delayed and low-precision gradient u_t^{s+1} .

Lemma 1. *If Assumptions 1, 2, 3 hold, then for the gradient u_t^{s+1} in Algorithm 1, its variance can be bounded by*

$$\mathbf{E} \|u_t^{s+1} - \nabla f(x_t^{s+1})\|^2 \leq 2L^2(\mu + 1)(\Delta + 2) \mathbf{E} [\|x_{D(t)}^{s+1} - x_t^{s+1}\|^2 + \|x_t^{s+1} - \tilde{x}^s\|^2],$$

where $\Delta = \frac{d}{4(2^{b-1}-1)^2}$.

Theorem 2. *Suppose $h(x)$ is convex, conditions in Lemma 1 hold, $T = Sm$, $\eta = \frac{\rho}{L}$, where $\rho \in (0, \frac{1}{2})$, and ρ, τ satisfy*

$$8\rho^2 m^2(\mu + 1)(\Delta + 2) + 2\rho^2(\mu + 1)(\Delta + 2)\tau^2 + \rho \leq 1. \quad (3)$$

Then, for the output x_{out} of Algorithm 1, we have

$$\mathbf{E} \|G_\eta(x_{out})\|^2 \leq \frac{2L(P(x^0) - P(x^*))}{\rho(1 - 2\rho)T}.$$

Remarks. From Theorem 2, we see that if $\mu = O(1)$, $b = O(\log \sqrt{d})$ and $\rho = O(\frac{1}{m})$, condition (3) can be easily satisfied, and AsyLPG achieves the same asymptotic convergence rate as in Theorem 1, while transmitting much fewer bits ($b = O(\log \sqrt{d})$ is much smaller than 32). The comparisons between QSVRG [2] and AsyLPG in Figure 3, 4 and Table 1 also validate that our model parameter quantization significantly reduces transmission time and bits. Note that AsyLPG can also adopt other gradient quantization methods (even biased ones), e.g., [27], and similar results can be established.

4.2 AsyLPG with Gradient Sparsification

In this section, we explore how to further reduce the communication cost by incorporating gradient sparsification into double quantization. As shown in Algorithm 2, in Steps 11-13, after calculating α_t , we successively perform sparsification and quantization on it. Specifically, we drop out certain coordinates of α_t to obtain a sparsified vector β_t according to the following rules [24]:

$$\beta_t = [Z_1 \frac{\alpha_{t,1}}{p_1}, Z_2 \frac{\alpha_{t,2}}{p_2}, \dots, Z_d \frac{\alpha_{t,d}}{p_d}], \quad (4)$$

where $Z = [Z_1, Z_2, \dots, Z_d]$ is a binary-valued vector with $Z_i \sim \text{Bernoulli}(p_i)$, $0 < p_i \leq 1$, and Z_i 's are independent. Thus, β_t is obtained by randomly selecting the i -th coordinate of α_t with probability p_i . It can be verified that $\mathbf{E}[\beta_t] = \alpha_t$. Define $\varphi_t \triangleq \sum_{i=1}^d p_i$ to measure the sparsity of β_t . To reduce the communication complexity, it is desirable to make φ_t as small as possible, which, on the other hand, brings about a large variance. The following lemma quantifies the relationship between β_t and φ_t , and is derived based on results in [22].

Lemma 2. *Suppose $\varphi_t \leq \frac{\|\alpha_t\|_1}{\|\alpha_t\|_\infty}$. Then, for $\alpha_t = \sum_{i=1}^d \alpha_{t,i} e_i$ and β_t generated in (4), we have $\mathbf{E} \|\beta_t\|^2 \geq \frac{1}{\varphi_t} \|\alpha_t\|_1^2$. The equality holds if and only if $p_i = \frac{|\alpha_{t,i}| \cdot \varphi_t}{\|\alpha_t\|_1}$.*

Based on Lemma 2, in Step 12 of Algorithm 2, we can choose a sparsity budget $\varphi_t \leq \frac{\|\alpha_t\|_1}{\|\alpha_t\|_\infty}$ and set $p_i = \frac{|\alpha_{t,i}| \cdot \varphi_t}{\|\alpha_t\|_1}$ to minimize the variance of β_t (since β_t is unbiased, its variance can be measured by the second moment). After obtaining β_t , in Step 13, we quantize it and send its low-precision version to the master. The model parameter x is updated in Step 9, in a similar manner as in Algorithm 1. In Algorithm 2, we also employ model parameter quantization and asynchronous parallelism in inner iterations.

Algorithm 2 Sparse-AsyLPG

```
1: Input:  $S, m, b_x, b, \eta, \tilde{x}^0 = x^0$ ;  
2: for  $s = 0, 1, \dots, S - 1$  do  
3:    $x_0^{s+1} = \tilde{x}^s$ ;  
4:   /* Map-reduce global gradient computation */  
5:   Compute  $\nabla f(\tilde{x}^s) = \frac{1}{n} \sum_{i=1}^n \nabla f_i(\tilde{x}^s)$ ;  
6:   for  $t = 0$  to  $m - 1$  do  
7:     /* For master: */  
8:     (i) Model Parameter Quantization: Set  $\delta_x = \frac{\|x_{D(t)}^{s+1}\|_\infty}{2^{b-1}-1}$  and quantize  $x_{D(t)}^{s+1}$  subject to (2). Send  $Q_{(\delta_x, b_x)}(x_{D(t)}^{s+1})$  to workers;  
9:     (ii) Receive local gradient  $\zeta_t$ , compute  $u_t^{s+1} = \zeta_t + \nabla f(\tilde{x}^s)$  and update  $x_{t+1}^{s+1} = \text{prox}_{\eta h}(x_t^{s+1} - \eta u_t^{s+1})$ ;  
10:    /* For worker: */  
11:    (i) Receive  $Q_{(\delta_x, b_x)}(x_{D(t)}^{s+1})$ , stochastically sample a data-point  $a \in \{1, \dots, n\}$ , and calculate gradient  $\alpha_t = \nabla f_a(Q_{(\delta_x, b_x)}(x_{D(t)}^{s+1})) - \nabla f_a(\tilde{x}^s)$ ;  
12:    (ii) Gradient Sparsification: Choose a sparsity budget  $\varphi_t$  and sparsify  $\alpha_t$  to obtain  $\beta_t$  using (4);  
13:    (iii) Gradient Quantization: Set  $\delta_{\beta_t} = \frac{\|\beta_t\|_\infty}{2^{b-1}-1}$ , and send  $\zeta_t = Q_{(\delta_{\beta_t}, b)}(\beta_t)$  to the master;  
14:  end for  
15:   $\tilde{x}^{s+1} = x_m^{s+1}$ ;  
16: end for  
17: Output: Uniformly choosing from  $\{x_t^{s+1}\}_{t=0}^{m-1}\}_{s=0}^{S-1}$ .
```

4.2.1 Theoretical Analysis

We first setup the variance of the sparsified gradient u_t^{s+1} .

Lemma 3. Suppose $\varphi_t \leq \frac{\|\alpha_t\|_1}{\|\alpha_t\|_\infty}$, Assumptions 1, 2, 3 hold, and for each $i \in \{1, \dots, d\}$, $p_i = \frac{|\alpha_{t,i}| \cdot \varphi_t}{\|\alpha_t\|_1}$. Denote $\Gamma = \frac{d^2}{4\varphi(2^{b-1}-1)^2} + \frac{d}{\varphi} + 1$, where $\varphi = \min_t \{\varphi_t\}$. Then, for the gradient u_t^{s+1} in Algorithm 2, we have

$$\mathbf{E} \|u_t^{s+1} - \nabla f(x_t^{s+1})\|^2 \leq 2L^2(\mu + 1)\Gamma [\mathbf{E} \|x_{D(t)}^{s+1} - x_t^{s+1}\|^2 + \|x_t^{s+1} - \tilde{x}^s\|^2].$$

Based on the above variance bound, we state the convergence behavior of Sparse-AsyLPG in the following theorem.

Theorem 3. Suppose $h(x)$ is convex, conditions in Lemma 3 hold, $T = Sm$, $\eta = \frac{\rho}{L}$, where $\rho \in (0, \frac{1}{2})$, and ρ, τ satisfy

$$8\rho^2 m^2 (\mu + 1)\Gamma + 2\rho^2 (\mu + 1)\tau^2 \Gamma + \rho \leq 1. \quad (5)$$

Then, for the output x_{out} of Algorithm 2, we have

$$\mathbf{E} \|G_\eta(x_{out})\|^2 \leq \frac{2L(P(x^0) - P(x^*))}{\rho(1 - 2\rho)T}. \quad (6)$$

Remarks. Setting $b = O(\log \sqrt{d})$, we obtain $\Gamma = O(d/\varphi)$. We can conclude from Theorem 3 that Sparse-AsyLPG converges with a rate linearly scales with \sqrt{d}/φ , and significantly reduces the number of transmitted bits per iteration. Note that before transmitting ζ_t , we need to encode it to a string, which contains 32 bits for δ_{β_t} and b bits for each coordinate. Since β_t is sparse, we only need to encode the nonzero coordinates, i.e., using $\log d$ bits to encode the position of a nonzero element followed by its value.

Algorithm 3 Acc-AsyLPG

```
1: Input:  $S, m, b_x, b, \tilde{x}^0, y_m^0 = \tilde{x}^0$ ;  
2: for  $s = 1, 2, \dots, S$  do  
3:   update  $\theta_s, \eta_s, x_0^s = \theta_s y_0^s + (1 - \theta_s) \tilde{x}^{s-1}, y_0^s = y_m^{s-1}$ ;  
4:   /* Map-reduce global gradient computation */  
5:   Compute  $\nabla f(\tilde{x}^{s-1}) = \frac{1}{n} \sum_{i=1}^n \nabla f_i(\tilde{x}^{s-1})$ ;  
6:   for  $t = 0$  to  $m - 1$  do  
7:     /* For master: */  
8:     (i) Model Parameter Quantization: Set  $\delta_x = \frac{\|x_{D(t)}^s\|_\infty}{2^{b-1}-1}$ , and quantize  $x_{D(t)}^s$  subject to (7). Then,  
       send  $Q_{(\delta_x, b_x)}(x_{D(t)}^s)$  to workers;  
9:     (ii) Momentum Acceleration:  
       Receive local gradient  $Q_{(\delta_{\alpha_t}, b)}(\alpha_t)$ ,  
       compute  $u_t^s = Q_{(\delta_{\alpha_t}, b)}(\alpha_t) + \nabla f(\tilde{x}^{s-1})$  and update  
        $y_{t+1}^s = \text{prox}_{\eta_s h}(y_t^s - \eta_s u_t^s)$ ,  
        $x_{t+1}^s = \tilde{x}^{s-1} + \theta_s (y_{t+1}^s - \tilde{x}^{s-1})$ ;  
10:    /* For worker: */  
11:    (i) Receive  $Q_{(\delta_x, b_x)}(x_{D(t)}^s)$ , stochastically sample a data-point  $a \in \{1, \dots, n\}$  and calculate gradient  
        $\alpha_t = \nabla f_a(Q_{(\delta_x, b_x)}(x_{D(t)}^s)) - \nabla f_a(\tilde{x}^{s-1})$ ;  
12:    (ii) Gradient Quantization: Set  $\delta_{\alpha_t} = \frac{\|\alpha_t\|_\infty}{2^{b-1}-1}$  and send the quantized gradient  $Q_{(\delta_{\alpha_t}, b)}(\alpha_t)$  to  
       the master;  
13:    end for  
14:     $\tilde{x}^s = \frac{1}{m} \sum_{t=0}^{m-1} x_{t+1}^s$ ;  
15:  end for  
16: Output:  $\tilde{x}^S$ .
```

4.3 Accelerated AsyLPG

In the above, we mainly focus on reducing the communication cost within each iteration. Here we propose an algorithm with an even faster convergence and fewer communication rounds. Specifically, we incorporate the popular momentum or Nesterov technique [14, 20] into AsyLPG. To simplify presentation, we only present accelerated AsyLPG (Acc-AsyLPG) in Algorithm 3. The method can similarly be applied to Sparse-AsyLPG.

Algorithm 3 still adopts asynchronous parallelism and double quantization, and makes the following key modifications: (i) in Step 8, the model parameter quantization satisfy

$$\mathbf{E}_Q \|Q_{(\delta_x, b_x)}(x_{D(t)}^s) - x_{D(t)}^s\|^2 \leq \theta_s \mu \|x_{D(t)}^s - \tilde{x}^{s-1}\|^2, \quad (7)$$

where μ is the hyperparameter that controls the precision loss. θ_s is the momentum weights and its value will be specified later. (ii) Momentum acceleration is implemented in Steps 3 and 9, through an auxiliary variable y_{t+1}^s . The update of x_{t+1}^s combines history information \tilde{x}^{s-1} and y_{t+1}^s .

In the following, we show that with the above modifications, Acc-AsyLPG achieves an even faster convergence rate.

Theorem 4. Suppose each $f_i(x)$ and $h(x)$ are convex, Assumptions 1, 2, 3 hold, and the domain Ω of x is bounded by D , such that $\forall x, y \in \Omega, \|x - y\|^2 \leq D$. Let $\theta_s = \frac{2}{s+2}$, $\eta_s = \frac{1}{\sigma L \theta_s}$, where $\sigma > 1$ is a constant.

If σ, τ satisfy $\tau \leq \frac{\sqrt{(\frac{2}{\gamma \theta_s} + \theta_s \Delta)^2 + \frac{4(\sigma-1)}{\gamma}} - (\frac{2}{\gamma \theta_s} + \theta_s \Delta)}{2}$ where $\Delta = \frac{d}{(2^{b-1}-1)^2} + 2$, $\gamma = 1 + 2\theta_s \mu$, then under Algorithm 3, we have

$$\mathbf{E}[P(\tilde{x}^S) - P(x^*)] \leq \tilde{O}((L/m + LD\mu\Delta/\tau + LD\mu)/S^2).$$

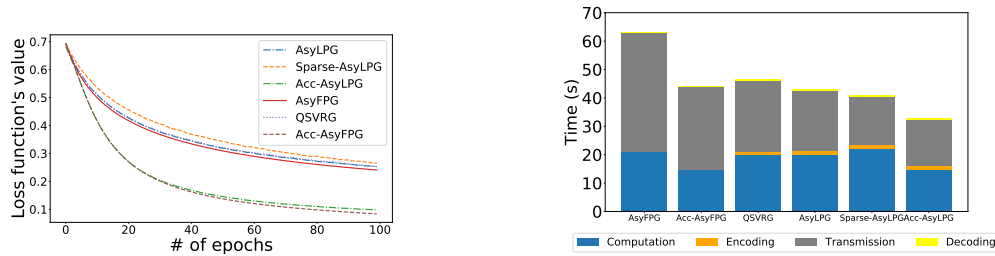


Figure 3: Comparison of six algorithms on dataset *real-sim*. Left: the training curve. Right: the decomposition of time consumption (the statistics are recorded until the training loss is first below 0.5).

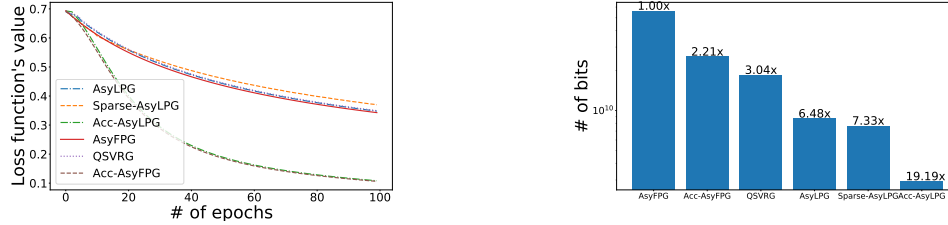


Figure 4: Comparison on dataset *rcv1*. Left: the training curve. Right: # of transmitted bits until the training loss is first below 0.4.

The bounded domain condition in Theorem 4 is commonly assumed in literature, e.g., [23], and the possibility of going outside domain is avoided by the proximal operator in Step 9. If $b = O(\log \sqrt{d})$ and $\mu = O(1)$, the constraint of delay τ can be easily satisfied with a moderate σ . Then, our Acc-AsyLPG achieves acceleration while effectively reducing the communication cost.

5 Experiments

We conduct experiments to validate the efficiency of our algorithms. The evaluations are setup on a 6-server distributed test-bed. Each server has 16 cores and 16GB memory. The communication between servers is handled by OpenMPI.²

5.1 Evaluations on Logistic Regression

We begin with logistic regression on dataset *real-sim* [5], and use L_1 , L_2 regularization with weights 10^{-5} and 10^{-4} respectively. The mini-batch size $B = 200$ and epoch length $m = \lceil \frac{n}{B} \rceil$. The following six algorithms are compared, using constant learning rate (denoted as lr) tuned to achieve the best result from $\{1e^{-1}, 1e^{-2}, 5e^{-2}, 1e^{-3}, 5e^{-3}, \dots, 1e^{-5}, 5e^{-5}\}$.

(i) AsyLPG, Sparse-AsyLPG, Acc-AsyLPG. We set $b_x = 8$ and $b = 8$ in these three algorithms. The sparsity budget in Sparse-AsyLPG is selected as $\varphi_t = \|\alpha_t\|_1 / \|\alpha_t\|_\infty$. We do not tune φ_t to present a fair comparison. Parameters in Acc-AsyLPG are set to be $\theta_s = 2/(s+2)$ and $\eta_s = lr/\theta_s$.

(ii) QSVRG [2], which is a gradient-quantized algorithm. We implement it in an asynchronous-parallelism way. Its gradient quantization method is equivalent to Step 12 in AsyLPG. If run with synchronization and without quantization, QSVRG and AsyLPG have the same convergence rate. For a fair comparison, we set the gradient quantization bit $b = 8$ for QSVRG.

(iii) The full-precision implementations of AsyLPG and Acc-AsyLPG, denoted as AsyFPG and Acc-AsyFPG, respectively. In both algorithms, we remove double quantization.

²<https://www.open-mpi.org/>

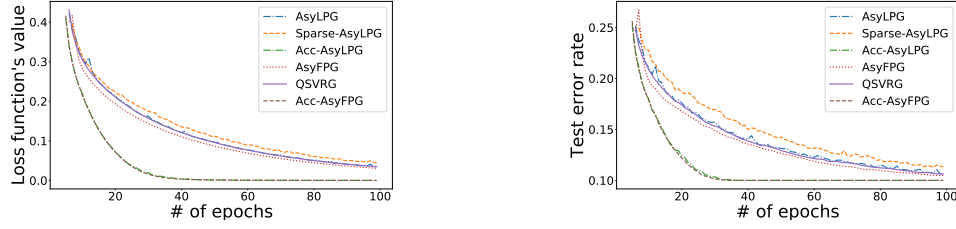


Figure 5: Comparison of six algorithms on dataset MNIST. Left: the training curve, right: the test error rate.

Algorithm	# bits	Ratio
AsyFPG	$2.42e9$	—
Acc-AsyFPG	$6.87e8$	$3.52\times$
QSVRG	$4.50e8$	$5.38\times$
AsyLPG	$3.33e8$	$7.28\times$
Sparse-AsyLPG	$2.73e8$	$8.87\times$
Acc-AsyLPG	$1.26e8$	$19.13\times$

μ	b_x	# bits	μ	b_x	# bits
0.005	11	$2.42e7$	2.0	6	$1.24e7$
0.01	10	$2.33e7$	10	5	$1.14e7$
0.05	9	$1.52e7$	50	4	$1.08e7$
0.1	8	$1.07e7$	150	3	$1.44e7$
0.5	7	$1.12e7$	800	2	$2.16e8$

Table 1: Evaluation on dataset MNIST. Left: # of transmitted bits until the training loss is first below 0.05. Right: The value of b_x and # of transmitted bits of AsyLPG under different μ .

Convergence and time consumption. Figure 3 shows the evaluations on dataset *real-sim*. The left plot shows that AsyLPG and Acc-AsyLPG have similar convergence rates to their full-precision counterparts. Our Sparse-AsyLPG also converges fast with little accuracy sacrifice. The time consumption presented in the right plot shows the communication-efficiency of our algorithms. With similar convergence rates, our low-precision algorithms significantly reduce the communication overhead when achieving the same training loss. Moreover, the comparison between AsyLPG and QSVRG validates the redundancy of 32 bits representation of model parameter.

Communication complexity. We experimented logistic regression on dataset *rcv1* [5]. The L_1 and L_2 regularization are adopted, both with weights 10^{-4} . lr is tuned in the same way as *real-sim*. In Figure 4, we record the total number of transmitted bits of the six algorithms. It shows that AsyLPG, Sparse-AsyLPG, Acc-AsyLPG can save up to $6.48\times$, $7.33\times$ and $19.19\times$ bits compared to AsyFPG.

5.2 Evaluations on Neural Network

We conduct evaluations on dataset MNIST³ using a 3-layer fully connected neural network. The hidden layer contains 100 nodes, and uses ReLU activation function. Softmax loss function and L_2 regularizer with weight 10^{-4} are adopted. We use 10k training samples and 2k test samples which are randomly drawn from the full dataset (60k training / 10k test). The mini-batch size is 20 and the epoch size m is 500. We set $b_x = 8$ and $b = 4$ for low-precision algorithms. lr is constant and is tuned to achieve the best result for each algorithm.

Figure 5 presents the convergence of the six algorithms. In the left table of Table 1, we record the total number of transmitted bits. We see that the results are similar as in the logistic regression case, i.e., our new low-precision algorithms can significantly reduce communication overhead compared to their full-precision counterparts and QSVRG.

Study of μ . The hyperparameter μ is set to control the precision loss incurred by model parameter quantization. Before, we fix b_x to compare our algorithms with other methods without model parameter quantization. In the right table of Table 1, we study the performance of AsyLPG under different μ . The value b_x is searched by guaranteeing (2). We provide the overall numbers of transmitted bits under different b_x

³<http://yann.lecun.com/exdb/mnist/>

until the training loss is first less than 0.5. The results validate that with the increasing μ , we can choose a smaller b_x , to save more communication cost per iteration. The total number of transmitted bits decreases until a threshold $\mu = 0.5$, beyond which significant precision loss happens and we need more training iterations for achieving the same accuracy.

6 Conclusion

We propose three communication-efficient algorithms for distributed training with asynchronous parallelism. The key idea is quantizing both model parameters and gradients, called double quantization. We analyze the variance of low-precision gradients and show that our algorithms achieve the same asymptotic convergence rate as the full-precision algorithms, while transmitting much fewer bits per iteration. We also incorporate gradient sparsification into double quantization, and setup relation between convergence rate and sparsity budget. We accelerate double quantization by integrating momentum technique. The evaluations on logistic regression and neural network validate that our algorithms can significantly reduce communication cost.

References

- [1] A. F. Aji and K. Heafield. Sparse communication for distributed gradient descent. *arXiv preprint arXiv:1704.05021*, 2017.
- [2] D. Alistarh, D. Grubic, J. Li, R. Tomioka, and M. Vojnovic. Qsgd: Communication-efficient sgd via gradient quantization and encoding. In *NeurIPS*, pages 1709–1720, 2017.
- [3] D. Alistarh, T. Hoefler, M. Johansson, N. Konstantinov, S. Khirirat, and C. Renggli. The convergence of sparsified gradient methods. In *NeurIPS*, pages 5977–5987, 2018.
- [4] R. Bekkerman, M. Bilenko, and J. Langford. *Scaling up machine learning: Parallel and distributed approaches*. Cambridge University Press, 2011.
- [5] C.-C. Chang and C.-J. Lin. Libsvm: a library for support vector machines. *ACM transactions on intelligent systems and technology (TIST)*, 2(3):27, 2011.
- [6] C. De Sa, M. Feldman, C. Ré, and K. Olukotun. Understanding and optimizing asynchronous low-precision stochastic gradient descent. In *ACM SIGARCH Computer Architecture News*, volume 45, pages 561–574. ACM, 2017.
- [7] C. De Sa, M. Leszczynski, J. Zhang, A. Marzoev, C. R. Aberger, K. Olukotun, and C. Ré. High-accuracy low-precision training. *arXiv preprint:1803.03383*, 2018.
- [8] J. Dean, G. Corrado, R. Monga, K. Chen, M. Devin, M. Mao, A. Senior, P. Tucker, K. Yang, Q. V. Le, et al. Large scale distributed deep networks. In *NeurIPS*, pages 1223–1231, 2012.
- [9] Z. Huo and H. Huang. Asynchronous stochastic gradient descent with variance reduction for non-convex optimization. *arXiv preprint arXiv:1604.03584*, 2016.
- [10] R. Johnson and T. Zhang. Accelerating stochastic gradient descent using predictive variance reduction. In *NeurIPS*, pages 315–323, 2013.
- [11] G. Lan. An optimal method for stochastic composite optimization. *Mathematical Programming*, 133(1-2):365–397, 2012.
- [12] X. Lian, Y. Huang, Y. Li, and J. Liu. Asynchronous parallel stochastic gradient for nonconvex optimization. In *NeurIPS*, pages 2737–2745, 2015.
- [13] A. Nedic and A. Ozdaglar. Distributed subgradient methods for multi-agent optimization. *IEEE Transactions on Automatic Control*, 54(1):48–61, 2009.
- [14] Y. Nesterov. A method of solving a convex programming problem with convergence rate $o(1/k^2)$. In *Soviet Mathematics Doklady*, volume 27, pages 372–376, 1983.
- [15] Y. Nesterov. *Introductory Lectures on Convex Optimization: A Basic Course*. Springer, 2003.
- [16] B. Recht, C. Re, S. Wright, and F. Niu. Hogwild: A lock-free approach to parallelizing stochastic gradient descent. In *NeurIPS*, pages 693–701, 2011.
- [17] S. J. Reddi, A. Hefny, S. Sra, B. Póczos, and A. J. Smola. On variance reduction in stochastic gradient descent and its asynchronous variants. In *NeurIPS*, pages 2647–2655, 2015.
- [18] S. J. Reddi, S. Sra, B. Póczos, and A. Smola. Fast stochastic methods for nonsmooth nonconvex optimization. In *NeurIPS*, 2016.

- [19] F. Seide, H. Fu, J. Droppo, G. Li, and D. Yu. 1-bit stochastic gradient descent and its application to data-parallel distributed training of speech dnns. In *Fifteenth Annual Conference of the International Speech Communication Association*, 2014.
- [20] F. Shang, Y. Liu, J. Cheng, and J. Zhuo. Fast stochastic variance reduced gradient method with momentum acceleration for machine learning. *arXiv preprint arXiv:1703.07948*, 2017.
- [21] S. U. Stich, J.-B. Cordonnier, and M. Jaggi. Sparsified sgd with memory. In *NeurIPS*, pages 4452–4463, 2018.
- [22] H. Wang, S. Sievert, Z. Charles, D. Papailiopoulos, and S. Wright. Atomo: Communication-efficient learning via atomic sparsification. In *NeurIPS*, 2018.
- [23] J. Wang, W. Wang, and N. Srebro. Memory and communication efficient distributed stochastic optimization with minibatch-prox. *Conference on Learning Theory (COLT)*, 2017.
- [24] J. Wangni, J. Wang, J. Liu, and T. Zhang. Gradient sparsification for communication-efficient distributed optimization. In *NeurIPS*, 2018.
- [25] W. Wen, C. Xu, F. Yan, C. Wu, Y. Wang, Y. Chen, and H. Li. Terngrad: Ternary gradients to reduce communication in distributed deep learning. In *NeurIPS*, pages 1509–1519, 2017.
- [26] J. Wu, W. Huang, J. Huang, and T. Zhang. Error compensated quantized sgd and its applications to large-scale distributed optimization. In *ICML*, 2018.
- [27] Y. Yu, J. Wu, and J. Huang. Exploring fast and communication-efficient algorithms in large-scale distributed networks. In *AISTATS*, 2019.
- [28] H. Zhang, J. Li, K. Kara, D. Alistarh, J. Liu, and C. Zhang. Zipml: Training linear models with end-to-end low precision, and a little bit of deep learning. In *ICML*, pages 4035–4043, 2017.

Supplementary Materials

7 Convergence Analysis for AsyLPG

Lemma 4. For a vector $v \in \mathbb{R}^d$, if $\delta = \frac{\|v\|_\infty}{2^{b-1}-1}$ or $\frac{\|v\|_2}{2^{b-1}-1}$, we have

$$\mathbf{E}\|Q_{(\delta,b)}(v) - v\|^2 \leq \frac{d\delta^2}{4}. \quad (8)$$

Proof. Because the squared L_2 norm separates along dimensions and each coordinate of v is independently quantized, we only need to prove $\mathbf{E}\|Q_{(\delta,b)}([v]_i) - [v]_i\|^2 \leq \frac{\delta^2}{4}$, for all $i \in \{1, \dots, d\}$. If the scaling factor $\delta = \frac{\|v\|_\infty}{2^{b-1}-1}$ or $\frac{\|v\|_2}{2^{b-1}-1}$, it can be verified that $[v]_i$ locates in the convex hull of $\text{dom}(\delta, b)$ and $Q_{(\delta,b)}(v)$ is an unbiased quantization. Then $\mathbf{E}\|Q_{(\delta,b)}([v]_i) - [v]_i\|^2 \leq \frac{\delta^2}{4}$ according to Lemma 1 in [27]. \square

Lemma 5. If Assumptions 1, 2, 3 hold, then for the gradient u_t^{s+1} in Algorithm 1, its variance can be bounded by

$$\mathbf{E}\|u_t^{s+1} - \nabla f(x_t^{s+1})\|^2 \leq 2L^2(\mu + 1)(\Delta + 2)\mathbf{E}[\|x_{D(t)}^{s+1} - x_t^{s+1}\|^2 + \|x_t^{s+1} - \tilde{x}^s\|^2], \quad (9)$$

where $\Delta = \frac{d}{4(2^{b-1}-1)^2}$.

Proof.

$$\begin{aligned} & \mathbf{E}\|u_t^{s+1} - \nabla f(x_t^{s+1})\|^2 \\ &= \mathbf{E}\|Q_{(\delta_{\alpha_t}, b)}(\alpha_t) + \nabla f(\tilde{x}^s) - \nabla f(x_t^{s+1})\|^2 \\ &= \mathbf{E}\|Q_{(\delta_{\alpha_t}, b)}(\alpha_t) - \alpha_t + \alpha_t + \nabla f(\tilde{x}^s) - \nabla f(x_t^{s+1})\|^2 \\ &= \mathbf{E}\|Q_{(\delta_{\alpha_t}, b)}(\alpha_t) - \alpha_t\|^2 + \mathbf{E}\|\alpha_t + \nabla f(\tilde{x}^s) - \nabla f(x_t^{s+1})\|^2 \\ &\leq \underbrace{\Delta \mathbf{E}\|\alpha_t\|^2}_{T_1} + \underbrace{\mathbf{E}\|\alpha_t + \nabla f(\tilde{x}^s) - \nabla f(x_t^{s+1})\|^2}_{T_2}, \end{aligned} \quad (10)$$

where the third equality holds because $\delta_{\alpha_t} = \frac{\|\alpha_t\|_\infty}{2^{b-1}-1}$ and $Q_{(\delta_{\alpha_t}, b)}(\alpha_t)$ is an unbiased quantization. The final inequality follows from Lemma 4. Next we bound T_1 and T_2 .

$$\begin{aligned} T_1 &= \mathbf{E}\|\nabla f_a(Q_{(\delta_x, b_x)}(x_{D(t)}^{s+1})) - \nabla f_a(\tilde{x}^s)\|^2 \\ &\leq L^2 \mathbf{E}\|Q_{(\delta_x, b_x)}(x_{D(t)}^{s+1}) - \tilde{x}^s\|^2 \\ &= L^2 \mathbf{E}\|Q_{(\delta_x, b_x)}(x_{D(t)}^{s+1}) - x_{D(t)}^{s+1}\|^2 + L^2 \mathbf{E}\|x_{D(t)}^{s+1} - \tilde{x}^s\|^2 \\ &\leq L^2(\mu + 1) \mathbf{E}\|x_{D(t)}^{s+1} - \tilde{x}^s\|^2 \\ &\leq 2L^2(\mu + 1) \mathbf{E}\|x_{D(t)}^{s+1} - x_t^{s+1}\|^2 + 2L^2(\mu + 1) \mathbf{E}\|x_t^{s+1} - \tilde{x}^s\|^2, \end{aligned} \quad (11)$$

where the first inequality adopts the Lipschitz smooth property of $f_a(x)$, and the second equality holds because $\delta_x = \frac{\|x_{D(t)}^{s+1}\|_\infty}{2^{b-1}-1}$ and $Q_{(\delta_x, b_x)}(x_{D(t)}^{s+1})$ is an unbiased quantization. The second inequality uses the condition in Step 8 of Algorithm 1. With similar arguments, we obtain the upper bound of T_2 in the following.

$$\begin{aligned}
T_2 &= \mathbf{E} \|\nabla f_a(Q_{(\delta_x, b_x)}(x_{D(t)}^{s+1})) - \nabla f_a(\tilde{x}^s) + \nabla f(\tilde{x}^s) - \nabla f(x_t^{s+1})\|^2 \\
&\leq 2\mathbf{E} \|\nabla f_a(Q_{(\delta_x, b_x)}(x_{D(t)}^{s+1})) - \nabla f_a(x_{D(t)}^{s+1})\|^2 + 2\mathbf{E} \|\nabla f_a(x_{D(t)}^{s+1}) - \nabla f_a(\tilde{x}^s) + \nabla f(\tilde{x}^s) - \nabla f(x_t^{s+1})\|^2 \\
&\leq 2\mathbf{E} \|\nabla f_a(Q_{(\delta_x, b_x)}(x_{D(t)}^{s+1})) - \nabla f_a(x_{D(t)}^{s+1})\|^2 + 4\mathbf{E} \|\nabla f_a(x_{D(t)}^{s+1}) - \nabla f_a(x_t^{s+1})\|^2 \\
&\quad + 4\mathbf{E} \|\nabla f_a(x_t^{s+1}) - \nabla f_a(\tilde{x}^s) + \nabla f(\tilde{x}^s) - \nabla f(x_t^{s+1})\|^2 \\
&\leq 2\mathbf{E} \|\nabla f_a(Q_{(\delta_x, b_x)}(x_{D(t)}^{s+1})) - \nabla f_a(x_{D(t)}^{s+1})\|^2 + 4\mathbf{E} \|\nabla f_a(x_{D(t)}^{s+1}) - \nabla f_a(x_t^{s+1})\|^2 + 4\mathbf{E} \|\nabla f_a(x_t^{s+1}) - \nabla f_a(\tilde{x}^s)\|^2 \\
&\leq 2L^2\mathbf{E} \|Q_{(\delta_x, b_x)}(x_{D(t)}^{s+1}) - x_{D(t)}^{s+1}\|^2 + 4L^2\mathbf{E} \|x_{D(t)}^{s+1} - x_t^{s+1}\|^2 + 4L^2\mathbf{E} \|x_t^{s+1} - \tilde{x}^s\|^2 \\
&\leq 4L^2(\mu + 1)\mathbf{E} \|x_{D(t)}^{s+1} - x_t^{s+1}\|^2 + 4L^2(\mu + 1)\mathbf{E} \|x_t^{s+1} - \tilde{x}^s\|^2.
\end{aligned} \tag{12}$$

where in the third inequality we adopt $\mathbf{E} \|\nabla f_a(x_t^{s+1}) - \nabla f_a(\tilde{x}^s) + \nabla f(\tilde{x}^s) - \nabla f(x_t^{s+1})\|^2 \leq \mathbf{E} \|\nabla f_a(x_t^{s+1}) - \nabla f_a(\tilde{x}^s)\|^2$. It is true because $\mathbf{E} \|x - \mathbf{E}[x]\|^2 \leq \mathbf{E} \|x\|^2$. The last inequality follows from Step 8 of Algorithm 1. Putting them together, we obtain Lemma 5. \square

Proof of Theorem 2. Define $\bar{x}_{t+1}^{s+1} \triangleq \text{prox}_{\eta h}(x_t^{s+1} - \eta \nabla f(x_t^{s+1}))$. According to equations (8)-(12) in [18], we get

$$\begin{aligned}
&\mathbf{E}[P(x_{t+1}^{s+1})] \\
&\leq \mathbf{E}[P(x_t^{s+1}) + (L - \frac{1}{2\eta})\|\bar{x}_{t+1}^{s+1} - x_t^{s+1}\|^2 + (\frac{L}{2} - \frac{1}{2\eta})\|x_{t+1}^{s+1} - x_t^{s+1}\|^2 - \frac{1}{2\eta}\|x_{t+1}^{s+1} - \bar{x}_{t+1}^{s+1}\|^2 \\
&\quad + \langle x_{t+1}^{s+1} - \bar{x}_{t+1}^{s+1}, \nabla f(x_t^{s+1}) - u_t^{s+1} \rangle] \\
&\leq \mathbf{E}[P(x_t^{s+1}) + \frac{\eta}{2}\|u_t^{s+1} - \nabla f(x_t^{s+1})\|^2 + (L - \frac{1}{2\eta})\|\bar{x}_{t+1}^{s+1} - x_t^{s+1}\|^2 + (\frac{L}{2} - \frac{1}{2\eta})\|x_{t+1}^{s+1} - x_t^{s+1}\|^2].
\end{aligned} \tag{13}$$

Using Lemma 5, we have

$$\begin{aligned}
\mathbf{E}[P(x_{t+1}^{s+1})] &\leq \mathbf{E}[P(x_t^{s+1}) + \eta L^2(\mu + 1)(\Delta + 2)\|x_{D(t)}^{s+1} - x_t^{s+1}\|^2 + \eta L^2(\mu + 1)(\Delta + 2)\|x_t^{s+1} - \tilde{x}^s\|^2 \\
&\quad + (L - \frac{1}{2\eta})\|\bar{x}_{t+1}^{s+1} - x_t^{s+1}\|^2 + (\frac{L}{2} - \frac{1}{2\eta})\|x_{t+1}^{s+1} - x_t^{s+1}\|^2].
\end{aligned} \tag{14}$$

Define $R_t^{s+1} \triangleq \mathbf{E}[P(x_t^{s+1}) + c_t\|x_t^{s+1} - \tilde{x}^s\|^2]$, where $\{c_t\}_{t=0}^m$ is a nonnegative decreasing sequence with $c_m = 0$, $c_t = c_{t+1}(1 + \beta) + \eta L^2(\mu + 1)(\Delta + 2)$ and $\beta = \frac{1}{m}$. Therefore,

$$\begin{aligned}
c_0 &\leq \eta L^2(\mu + 1)(\Delta + 2) \cdot \frac{(1 + \beta)^m - 1}{\beta} \\
&\leq 2\eta L^2(\mu + 1)(\Delta + 2)m.
\end{aligned} \tag{15}$$

From the definition of R_t^{s+1} , we obtain

$$\begin{aligned}
R_{t+1}^{s+1} &= \mathbf{E}[P(x_{t+1}^{s+1}) + c_{t+1}\|x_{t+1}^{s+1} - \tilde{x}^s\|^2] \\
&\leq \mathbf{E}[P(x_{t+1}^{s+1}) + c_{t+1}(1 + \frac{1}{\beta})\|x_{t+1}^{s+1} - x_t^{s+1}\|^2 + c_{t+1}(1 + \beta)\|x_t^{s+1} - \tilde{x}^s\|^2] \\
&\leq \mathbf{E}[P(x_t^{s+1}) + c_t\|x_t^{s+1} - \tilde{x}^s\|^2 + (c_{t+1}(1 + \frac{1}{\beta}) + \frac{L}{2} - \frac{1}{2\eta})\|x_{t+1}^{s+1} - x_t^{s+1}\|^2 + (L - \frac{1}{2\eta})\|\bar{x}_{t+1}^{s+1} - x_t^{s+1}\|^2 \\
&\quad + \eta L^2(\mu + 1)(\Delta + 2)\tau \sum_{d=D(t)}^{t-1} \|x_{d+1}^{s+1} - x_d^{s+1}\|^2].
\end{aligned} \tag{16}$$

Summing over $t = 0$ to $m - 1$, we get

$$\begin{aligned} \sum_{t=0}^{m-1} R_{t+1}^{s+1} &\leq \sum_{t=0}^{m-1} R_t^{s+1} + \sum_{t=0}^{m-1} [c_{t+1}(1 + \frac{1}{\beta}) + \frac{L}{2} - \frac{1}{2\eta} + \eta L^2(\mu + 1)(\Delta + 2)\tau^2] \mathbf{E} \|x_{t+1}^{s+1} - x_t^{s+1}\|^2 \\ &\quad + \sum_{t=0}^{m-1} (L - \frac{1}{2\eta}) \mathbf{E} \|\bar{x}_{t+1}^{s+1} - x_t^{s+1}\|^2. \end{aligned} \quad (17)$$

The inequality holds because $\sum_{t=0}^{m-1} \sum_{d=D(t)}^{t-1} \|x_{d+1}^{s+1} - x_d^{s+1}\|^2 \leq \tau \sum_{t=0}^{m-1} \|x_{t+1}^{s+1} - x_t^{s+1}\|^2$.

Now we derive the bound for η to make $[c_{t+1}(1 + \frac{1}{\beta}) + \frac{L}{2} - \frac{1}{2\eta} + \eta L^2(\mu + 1)(\Delta + 2)\tau^2] \leq 0$. Since c_t is a decreasing sequence, we only need to prove the above inequality for c_0 . Let $\eta = \frac{\rho}{L}$, where $\rho < \frac{1}{2}$ is a positive constant. After calculations, we obtain the following constraint:

$$8\rho^2 m^2(\mu + 1)(\Delta + 2) + 2\rho^2(\mu + 1)(\Delta + 2)\tau^2 + \rho \leq 1. \quad (18)$$

If (18) holds, then

$$\sum_{t=0}^{m-1} R_{t+1}^{s+1} \leq \sum_{t=0}^{m-1} R_t^{s+1} + (L - \frac{1}{2\eta}) \sum_{t=0}^{m-1} \mathbf{E} \|\bar{x}_{t+1}^{s+1} - x_t^{s+1}\|^2. \quad (19)$$

Because $x_0^{s+1} = \tilde{x}^s$, $x_m^{s+1} = \tilde{x}^{s+1}$ and $c_m = 0$, we have $R(x_0^{s+1}) = P(\tilde{x}^s)$ and $R(x_m^{s+1}) = P(\tilde{x}^{s+1})$. Summing (19) over $s = 0$ to $S - 1$, we get

$$(\frac{1}{2\eta} - L) \sum_{s=0}^{S-1} \sum_{t=0}^{m-1} \mathbf{E} \|\bar{x}_{t+1}^{s+1} - x_t^{s+1}\|^2 \leq P(x^0) - P(x^*). \quad (20)$$

Using the definition of $G_\eta(x_t^{s+1}) \triangleq \frac{1}{\eta}[x_t^{s+1} - \text{prox}_{\eta h}(x_t^{s+1} - \eta \nabla f(x_t^{s+1}))] = \frac{1}{\eta}(x_t^{s+1} - \bar{x}_{t+1}^{s+1})$, we obtain Theorem 2. \square

8 Analysis for Sparse-AsyLPG

Lemma 6. Define $\varphi_t \triangleq \sum_{i=1}^d p_i$. If $\varphi_t \leq \frac{\|\alpha_t\|_1}{\|\alpha_t\|_\infty}$, then for $\alpha_t = \sum_{i=1}^d \alpha_{t,i} e_i$, we have $\mathbf{E} \|\beta_t\|^2 \geq \frac{1}{\varphi_t} \|\alpha_t\|_1^2$. The equality holds if and only if $p_i = \frac{|\alpha_{t,i}| \cdot \varphi_t}{\|\alpha_t\|_1}$.

Proof Sketch. From the calculation of β_t , we obtain $\mathbf{E} \|\beta_t\|^2 = \sum_{i=1}^d \frac{\alpha_{t,i}^2}{p_i}$. If $\varphi_t \leq \frac{\|\alpha_t\|_1}{\|\alpha_t\|_\infty}$, then it can be concluded from Lemma 3 and Theorem 5 in [22] that $\mathbf{E} \|\beta_t\|^2 \geq \frac{1}{\varphi_t} \|\alpha_t\|_1^2$, with equality if and only if $p_i = \frac{|\alpha_{t,i}| \cdot \varphi_t}{\|\alpha_t\|_1}$. \square

Lemma 7. Suppose $\varphi_t \leq \frac{\|\alpha_t\|_1}{\|\alpha_t\|_\infty}$. Assumptions 1, 2, 3 hold and for each $i \in \{1, \dots, d\}$, $p_i = \frac{|\alpha_{t,i}| \cdot \varphi_t}{\|\alpha_t\|_1}$. Denote $\Gamma = \frac{d^2}{4\varphi(2^b-1)^2} + \frac{d}{\varphi} + 1$, where $\varphi = \min_t \{\varphi_t\}$. Then, for the gradient u_t^{s+1} in Algorithm 2, we have

$$\mathbf{E} \|u_t^{s+1} - \nabla f(x_t^{s+1})\|^2 \leq 2L^2(\mu + 1)\Gamma[\mathbf{E} \|x_{D(t)}^{s+1} - x_t^{s+1}\|^2 + \|x_t^{s+1} - \tilde{x}^s\|^2]. \quad (21)$$

Proof.

$$\begin{aligned}
& \mathbf{E} \|u_t^{s+1} - \nabla f(x_t^{s+1})\|^2 \\
&= \mathbf{E} \|Q_{(\delta_{\beta_t}, b)}(\beta_t) + \nabla f(\tilde{x}^s) - \nabla f(x_t^{s+1})\|^2 \\
&= \mathbf{E} \|Q_{(\delta_{\beta_t}, b)}(\beta_t) - \beta_t\|^2 + \mathbf{E} \|\beta_t + \nabla f(\tilde{x}^s) - \nabla f(x_t^{s+1})\|^2 \\
&\leq \frac{d}{4(2^{b-1} - 1)^2} \mathbf{E} \|\beta_t\|^2 + \mathbf{E} \|\beta_t - \alpha_t\|^2 + \mathbf{E} \|\alpha_t + \nabla f(\tilde{x}^s) - \nabla f(x_t^{s+1})\|^2 \\
&= \left[\frac{d}{4(2^{b-1} - 1)^2} + 1 \right] \mathbf{E} \|\beta_t\|^2 - \mathbf{E} \|\alpha_t\|^2 + \mathbf{E} \|\alpha_t + \nabla f(\tilde{x}^s) - \nabla f(x_t^{s+1})\|^2
\end{aligned} \tag{22}$$

where the second equality holds because $Q_{(\delta_{\beta_t}, b)}(\beta_t)$ is an unbiased quantization. The first inequality uses Lemma 4 and $\mathbf{E}[\beta_t] = \alpha_t$. According to T_2 we get

$$\begin{aligned}
& \mathbf{E} \|u_t^{s+1} - \nabla f(x_t^{s+1})\|^2 \\
&\leq \left[\frac{d}{4(2^{b-1} - 1)^2} + 1 \right] \mathbf{E} \|\beta_t\|^2 - \mathbf{E} \|\alpha_t\|^2 + 4L^2(\mu + 1) \mathbf{E} \|x_{D(t)}^{s+1} - x_t^{s+1}\|^2 + 4L^2(\mu + 1) \mathbf{E} \|x_t^{s+1} - \tilde{x}^s\|^2.
\end{aligned} \tag{23}$$

From Lemma 6, we obtain

$$\begin{aligned}
& \mathbf{E} \|u_t^{s+1} - \nabla f(x_t^{s+1})\|^2 \\
&\leq \left[\frac{d^2}{4\varphi(2^{b-1} - 1)^2} + \frac{d}{\varphi} - 1 \right] \mathbf{E} \|\alpha_t\|^2 + 4L^2(\mu + 1) \mathbf{E} \|x_{D(t)}^{s+1} - x_t^{s+1}\|^2 + 4L^2(\mu + 1) \mathbf{E} \|x_t^{s+1} - \tilde{x}^s\|^2 \\
&\leq 2L^2(\mu + 1) \left[\frac{d^2}{4\varphi(2^{b-1} - 1)^2} + \frac{d}{\varphi} + 1 \right] \mathbf{E} \|x_{D(t)}^{s+1} - x_t^{s+1}\|^2 + 2L^2(\mu + 1) \left[\frac{d^2}{4\varphi(2^{b-1} - 1)^2} + \frac{d}{\varphi} + 1 \right] \mathbf{E} \|x_t^{s+1} - \tilde{x}^s\|^2,
\end{aligned} \tag{24}$$

where the first inequality uses $\|x\|_1 \leq \sqrt{d}\|x\|_2$ for $x \in \mathbb{R}^d$ and $\mathbf{E} \|\beta_t\|^2 = \frac{1}{\varphi_t} \|\alpha_t\|_1^2$ when $p_i = \frac{|\alpha_{t,i}| \cdot \varphi_t}{\|\alpha_t\|_1}$. The final inequality comes from the upper bound of T_1 . \square

Proof sketch of Theorem 3. Substituting (21) in (13) and following the proof of Theorem 2, we obtain a convergence rate of

$$\mathbf{E} \|G_\eta(x_{out})\|^2 \leq \frac{2L[P(x^0) - P(x^*)]}{\rho(1 - 2\rho)T}, \tag{25}$$

if $8\rho^2 m^2(\mu + 1)\Gamma + 2\rho^2(\mu + 1)\tau^2\Gamma + \rho \leq 1$, where $\Gamma = \frac{d^2}{4\varphi(2^{b-1} - 1)^2} + \frac{d}{\varphi} + 1$. \square

9 Proof of Theorem 4

The following lemma is a widely used technical result in composite optimization, which is called *3-Point-Property*. Lemma 1 in [11] provides its detailed proofs and extensions.

Lemma 8. *If y_{t+1}^s is the optimal solution of*

$$\min_{y \in \chi} \phi(y) + \frac{1}{2\eta_s} \|y - y_t^s\|^2, \tag{26}$$

where function $\phi(y)$ is convex over a convex set χ . Then for any $y \in \chi$, we have [11]

$$\phi(y) + \frac{1}{2\eta_s} \|y - y_t^s\|^2 \geq \phi(y_{t+1}^s) + \frac{1}{2\eta_s} \|y_{t+1}^s - y_t^s\|^2 + \frac{1}{2\eta_s} \|y - y_{t+1}^s\|^2. \tag{27}$$

Proof of Theorem 4. From the update rule of y_{t+1}^s , we know that

$$y_{t+1}^s = \arg \min_y h(y) + \langle u_t^s, y - y_t^s \rangle + \frac{1}{2\eta_s} \|y - y_t^s\|^2. \quad (28)$$

Applying Lemma 8 with $\phi(y) = h(y) + \langle u_t^s, y - y_t^s \rangle$ and $y = x^*$ in (27), we obtain

$$h(y_{t+1}^s) + \langle u_t^s, y_{t+1}^s - y_t^s \rangle \leq h(x^*) + \langle u_t^s, x^* - y_t^s \rangle + \frac{1}{2\eta_s} \|x^* - y_t^s\|^2 - \frac{1}{2\eta_s} \|x^* - y_{t+1}^s\|^2 - \frac{1}{2\eta_s} \|y_{t+1}^s - y_t^s\|^2. \quad (29)$$

Since $f(x)$ is Lipschitz smooth, we have

$$\begin{aligned} \mathbf{E}f(x_{t+1}^s) &\leq \mathbf{E}(f(x_t^s) + \langle \nabla f(x_t^s), x_{t+1}^s - x_t^s \rangle + \frac{L}{2} \|x_{t+1}^s - x_t^s\|^2) \\ &= \mathbf{E}(f(x_t^s) + \theta_s \langle u_t^s, y_{t+1}^s - y_t^s \rangle + \theta_s \langle \nabla f(x_t^s) - u_t^s, y_{t+1}^s - y_t^s \rangle + \frac{L}{2} \|x_{t+1}^s - x_t^s\|^2), \end{aligned} \quad (30)$$

where the first equality uses $x_{t+1}^s - x_t^s = \theta_s(y_{t+1}^s - y_t^s)$. Therefore,

$$\begin{aligned} \mathbf{E}P(x_{t+1}^s) &= \mathbf{E}[f(x_{t+1}^s) + h(x_{t+1}^s)] \\ &\leq \mathbf{E}[f(x_t^s) + \theta_s \langle u_t^s, y_{t+1}^s - y_t^s \rangle + \theta_s \langle \nabla f(x_t^s) - u_t^s, y_{t+1}^s - y_t^s \rangle + \frac{L}{2} \|x_{t+1}^s - x_t^s\|^2 + h(x_{t+1}^s)] \\ &\leq \mathbf{E}[f(x_t^s) + \theta_s \langle u_t^s, y_{t+1}^s - y_t^s \rangle + \theta_s \langle \nabla f(x_t^s) - u_t^s, y_{t+1}^s - y_t^s \rangle + \frac{L}{2} \|x_{t+1}^s - x_t^s\|^2 + (1 - \theta_s)h(\tilde{x}^{s-1}) + \theta_s h(y_{t+1}^s)] \\ &\leq \mathbf{E}[\theta_s h(x^*) + \underbrace{\theta_s \langle u_t^s, x^* - y_t^s \rangle}_{T_3} + \frac{\theta_s}{2\eta_s} \|x^* - y_t^s\|^2 - \frac{\theta_s}{2\eta_s} \|x^* - y_{t+1}^s\|^2 - \frac{\theta_s}{2\eta_s} \|y_{t+1}^s - y_t^s\|^2 \\ &\quad + f(x_t^s) + \underbrace{\theta_s \langle \nabla f(x_t^s) - u_t^s, y_{t+1}^s - y_t^s \rangle}_{T_4} + \frac{L}{2} \|x_{t+1}^s - x_t^s\|^2 + (1 - \theta_s)h(\tilde{x}^{s-1})], \end{aligned} \quad (31)$$

where the first inequality uses (30), and the second inequality follows from $x_{t+1}^s = \theta_s y_{t+1}^s + (1 - \theta_s)\tilde{x}^{s-1}$ and the convexity of $h(x)$. We apply (29) in the third inequality. T_3 can be bounded as follows.

$$\begin{aligned} \mathbf{E}T_3 &= \theta_s \mathbf{E}\langle u_t^s, x^* - y_t^s \rangle \\ &= \mathbf{E}\langle u_t^s, \theta_s x^* + (1 - \theta_s)\tilde{x}^{s-1} - x_t^s \rangle \\ &= \mathbf{E}\langle u_t^s, \theta_s x^* + (1 - \theta_s)\tilde{x}^{s-1} - Q_{(\delta_x, b_x)}(x_{D(t)}^s) \rangle + \mathbf{E}\langle u_t^s, Q_{(\delta_x, b_x)}(x_{D(t)}^s) - x_t^s \rangle \\ &= \mathbf{E}\langle \nabla f_a(Q_{(\delta_x, b_x)}(x_{D(t)}^s)), \theta_s x^* + (1 - \theta_s)\tilde{x}^{s-1} - Q_{(\delta_x, b_x)}(x_{D(t)}^s) \rangle + \mathbf{E}\langle \nabla f_a(Q_{(\delta_x, b_x)}(x_{D(t)}^s)), Q_{(\delta_x, b_x)}(x_{D(t)}^s) - x_t^s \rangle \\ &\leq \mathbf{E}[f_a(\theta_s x^* + (1 - \theta_s)\tilde{x}^{s-1}) - f_a(Q_{(\delta_x, b_x)}(x_{D(t)}^s)) + f_a(Q_{(\delta_x, b_x)}(x_{D(t)}^s)) - f_a(x_t^s) + \frac{L}{2} \|Q_{(\delta_x, b_x)}(x_{D(t)}^s) - x_t^s\|^2] \\ &\leq \mathbf{E}[\theta_s f(x^*) + (1 - \theta_s)f(\tilde{x}^{s-1}) - f(x_t^s) + \frac{L}{2} \|Q_{(\delta_x, b_x)}(x_{D(t)}^s) - x_t^s\|^2], \end{aligned} \quad (32)$$

where the convexity and Lipschitz smoothness of $f_a(x)$ are adopted in the first inequality. Next we derive the bound of $\mathbf{E}\|Q_{(\delta_x, b_x)}(x_{D(t)}^s) - x_t^s\|^2$ as follows.

$$\begin{aligned} \mathbf{E}\|Q_{(\delta_x, b_x)}(x_{D(t)}^s) - x_t^s\|^2 &= \mathbf{E}\|Q_{(\delta_x, b_x)}(x_{D(t)}^s) - x_{D(t)}^s\|^2 + \mathbf{E}\|x_{D(t)}^s - x_t^s\|^2 \\ &\leq \theta_s \mu \mathbf{E}\|x_{D(t)}^s - \tilde{x}^{s-1}\|^2 + \mathbf{E}\|x_{D(t)}^s - x_t^s\|^2 \\ &\leq (1 + 2\theta_s \mu) \mathbf{E}\|x_{D(t)}^s - x_t^s\|^2 + 2\theta_s^3 \mu \mathbf{E}\|y_t^s - \tilde{x}^{s-1}\|^2 \\ &\leq (1 + 2\theta_s \mu) \mathbf{E}\|x_{D(t)}^s - x_t^s\|^2 + 2\theta_s^3 \mu D. \end{aligned} \quad (33)$$

where the first equality holds because $Q_{(\delta_x, b_x)}(x_{D(t)}^s)$ is an unbiased quantization and the first inequality comes from Step 8 in Algorithm 3. The second inequality holds because $x_t^s - \tilde{x}^{s-1} = \theta_s(y_t^s - \tilde{x}^{s-1})$. Therefore,

$$\mathbf{E}T_3 \leq \mathbf{E}[\theta_s f(x^*) + (1 - \theta_s)f(\tilde{x}^{s-1}) - f(x_t^s) + \frac{(1 + 2\theta_s\mu)L}{2} \|x_{D(t)}^s - x_t^s\|^2 + \theta_s^3\mu LD]. \quad (34)$$

Now we bound T_4 . Define $v_t^s \triangleq \nabla f_a(x_t^s) - \nabla f_a(\tilde{x}^{s-1}) + \nabla f(\tilde{x}^{s-1})$.

$$\mathbf{E}T_4 = \theta_s \mathbf{E}\langle \nabla f(x_t^s) - u_t^s, y_{t+1}^s - y_t^s \rangle = \underbrace{\theta_s \mathbf{E}\langle \nabla f(x_t^s) - v_t^s, y_{t+1}^s - y_t^s \rangle}_{T_5} + \underbrace{\theta_s \mathbf{E}\langle v_t^s - u_t^s, y_{t+1}^s - y_t^s \rangle}_{T_6}. \quad (35)$$

$$\begin{aligned} T_5 &= \theta_s \mathbf{E}\langle \nabla f(x_t^s) - v_t^s, y_{t+1}^s - y_t^s \rangle \\ &\leq \frac{\theta_s}{2\tau L} \mathbf{E}\|\nabla f(x_t^s) - v_t^s\|^2 + \frac{\tau L \theta_s}{2} \mathbf{E}\|y_{t+1}^s - y_t^s\|^2 \\ &\leq \frac{\theta_s}{2\tau L} \mathbf{E}\|\nabla f_a(x_t^s) - \nabla f_a(\tilde{x}^{s-1})\|^2 + \frac{\tau L \theta_s}{2} \mathbf{E}\|y_{t+1}^s - y_t^s\|^2 \\ &\leq \frac{\theta_s L^2}{2\tau L} \mathbf{E}\|x_t^s - \tilde{x}^{s-1}\|^2 + \frac{\tau L \theta_s}{2} \mathbf{E}\|y_{t+1}^s - y_t^s\|^2 \\ &= \frac{\theta_s^3 L^2}{2\tau L} \mathbf{E}\|y_t^s - \tilde{x}^{s-1}\|^2 + \frac{\tau L \theta_s}{2} \mathbf{E}\|y_{t+1}^s - y_t^s\|^2 \\ &\leq \frac{\theta_s^3 LD}{2\tau} + \frac{\tau L \theta_s}{2} \mathbf{E}\|y_{t+1}^s - y_t^s\|^2, \end{aligned} \quad (36)$$

where in the first inequality we use Young's inequality. The second equality follows from $x_t^s - \tilde{x}^{s-1} = \theta_s(y_t^s - \tilde{x}^{s-1})$. Moreover,

$$\begin{aligned} T_6 &= \theta_s \mathbf{E}\langle v_t^s - u_t^s, y_{t+1}^s - y_t^s \rangle \\ &\leq \frac{\theta_s}{2\tau L} \mathbf{E}\|v_t^s - u_t^s\|^2 + \frac{\tau L \theta_s}{2} \mathbf{E}\|y_{t+1}^s - y_t^s\|^2. \end{aligned} \quad (37)$$

From the definition of u_t^s and v_t^s , we have

$$\begin{aligned}
& \mathbf{E} \|v_t^s - u_t^s\|^2 \\
&= \mathbf{E} \|Q_{(\delta_{\alpha_t}, b)}(\alpha_t) - \nabla f_a(x_t^s) + \nabla f_a(\tilde{x}^{s-1})\|^2 \\
&= \mathbf{E} \|Q_{(\delta_{\alpha_t}, b)}(\nabla f_a(Q_{(\delta_x, b_x)}(x_{D(t)}^s)) - \nabla f_a(\tilde{x}^{s-1})) - \nabla f_a(Q_{(\delta_x, b_x)}(x_{D(t)}^s)) + \nabla f_a(\tilde{x}^{s-1})\|^2 \\
&\quad + \mathbf{E} \|\nabla f_a(Q_{(\delta_x, b_x)}(x_{D(t)}^s)) - \nabla f_a(x_t^s)\|^2 \\
&\leq \frac{d}{4(2^{b-1} - 1)^2} \mathbf{E} \|\nabla f_a(Q_{(\delta_x, b_x)}(x_{D(t)}^s)) - \nabla f_a(\tilde{x}^{s-1})\|^2 + \mathbf{E} \|\nabla f_a(Q_{(\delta_x, b_x)}(x_{D(t)}^s)) - \nabla f_a(x_t^s)\|^2 \\
&\leq \frac{dL^2}{4(2^{b-1} - 1)^2} \mathbf{E} \|Q_{(\delta_x, b_x)}(x_{D(t)}^s) - \tilde{x}^{s-1}\|^2 + L^2 \mathbf{E} \|Q_{(\delta_x, b_x)}(x_{D(t)}^s) - x_t^s\|^2 \\
&\leq [\frac{dL^2}{2(2^{b-1} - 1)^2} + L^2] \mathbf{E} \|Q_{(\delta_x, b_x)}(x_{D(t)}^s) - x_t^s\|^2 + \frac{dL^2}{2(2^{b-1} - 1)^2} \mathbf{E} \|x_t^s - \tilde{x}^{s-1}\|^2 \\
&\leq [\frac{dL^2}{(2^{b-1} - 1)^2} + 2L^2] \mathbf{E} \|Q_{(\delta_x, b_x)}(x_{D(t)}^s) - x_{D(t)}^s\|^2 + [\frac{dL^2}{(2^{b-1} - 1)^2} + 2L^2] \mathbf{E} \|x_{D(t)}^s - x_t^s\|^2 \\
&\quad + \frac{dL^2\theta_s^2}{2(2^{b-1} - 1)^2} \mathbf{E} \|y_t^s - \tilde{x}^{s-1}\|^2 \\
&\leq [\frac{dL^2}{(2^{b-1} - 1)^2} + 2L^2] \theta_s \mu \mathbf{E} \|x_{D(t)}^s - \tilde{x}^{s-1}\|^2 + [\frac{dL^2}{(2^{b-1} - 1)^2} + 2L^2] \mathbf{E} \|x_{D(t)}^s - x_t^s\|^2 + \frac{dL^2\theta_s^2 D}{2(2^{b-1} - 1)^2} \\
&\leq [\frac{dL^2}{(2^{b-1} - 1)^2} + 2L^2] (1 + 2\theta_s \mu) \mathbf{E} \|x_{D(t)}^s - x_t^s\|^2 + [\frac{2dL^2}{(2^{b-1} - 1)^2} + 4L^2] \theta_s \mu \mathbf{E} \|x_t^s - \tilde{x}^{s-1}\|^2 + \frac{dL^2\theta_s^2 D}{2(2^{b-1} - 1)^2} \\
&\leq (1 + 2\theta_s \mu) L^2 [\frac{d}{(2^{b-1} - 1)^2} + 2] \mathbf{E} \|x_{D(t)}^s - x_t^s\|^2 + \theta_s^3 L^2 \mu [\frac{2d}{(2^{b-1} - 1)^2} + 4] D + \frac{dL^2\theta_s^2 D}{2(2^{b-1} - 1)^2},
\end{aligned} \tag{38}$$

where the second equality holds because $Q_{(\delta_{\alpha_t}, b)}(\alpha_t)$ is an unbiased quantization, and the first inequality uses Lemma 4. In the fourth and final inequality, we adopt $x_t^s - \tilde{x}^{s-1} = \theta_s(y_t^s - \tilde{x}^{s-1})$. The fifth inequality follows from Step 8 of Algorithm 3. Putting them together, we obtain

$$\begin{aligned}
\mathbf{E} T_4 &\leq \tau L \theta_s \mathbf{E} \|y_{t+1}^s - y_t^s\|^2 + \frac{L \theta_s (1 + 2\theta_s \mu)}{2\tau} [\frac{d}{(2^{b-1} - 1)^2} + 2] \mathbf{E} \|x_{D(t)}^s - x_t^s\|^2 + \frac{LD\theta_s^3}{2\tau} [\frac{d}{2(2^{b-1} - 1)^2} + 1] \\
&\quad + \frac{\theta_s^4 LD\mu}{2\tau} [\frac{2d}{(2^{b-1} - 1)^2} + 4].
\end{aligned} \tag{39}$$

Substituting (39) and (34) in (31), we get

$$\begin{aligned}
\mathbf{E} P(x_{t+1}^s) &\leq \mathbf{E} [(1 - \theta_s)P(\tilde{x}^{s-1}) + \theta_s P(x^*) + \frac{\theta_s}{2\eta_s} (\|x^* - y_t^s\|^2 - \|x^* - y_{t+1}^s\|^2) \\
&\quad + \theta_s^3 \mu LD + \frac{LD\theta_s^3}{2\tau} [\frac{d}{2(2^{b-1} - 1)^2} + 1] + \frac{\theta_s^4 LD\mu}{2\tau} [\frac{2d}{(2^{b-1} - 1)^2} + 4] \\
&\quad + \underbrace{\frac{(1 + 2\theta_s \mu)L}{2} \|x_{D(t)}^s - x_t^s\|^2 + \tau L \theta_s \|y_{t+1}^s - y_t^s\|^2 + \frac{L \theta_s (1 + 2\theta_s \mu)}{2\tau} [\frac{d}{(2^{b-1} - 1)^2} + 2] \|x_{D(t)}^s - x_t^s\|^2}_{T_7} \\
&\quad + \underbrace{\frac{L}{2} \|x_{t+1}^s - x_t^s\|^2 - \frac{\theta_s}{2\eta_s} \|y_{t+1}^s - y_t^s\|^2}_{T_8}].
\end{aligned} \tag{40}$$

Let $\eta_s \theta_s = \frac{1}{\sigma L}$ where $\sigma > 1$, since $\sum_{t=0}^{m-1} \sum_{d=D(t)}^{t-1} \|x_{d+1}^s - x_d^s\|^2 \leq \tau \sum_{t=0}^{m-1} \|x_{t+1}^s - x_t^s\|^2$, it can be verified that

$$\sum_{t=0}^{m-1} (T_7 + T_8) \leq \xi \sum_{t=0}^{m-1} \|y_{t+1}^s - y_t^s\|^2, \quad (41)$$

where $\xi = \tau^2 \theta_s^2 \left[\frac{(1+2\theta_s \mu)L}{2} + \frac{(1+2\theta_s \mu)\theta_s L}{2\tau} \left(\frac{d}{(2^{b-1}-1)^2} + 2 \right) \right] + \tau L \theta_s + \frac{L\theta_s^2}{2} - \frac{\sigma L \theta_s^2}{2}$. Denote $\Delta = \frac{d}{(2^{b-1}-1)^2} + 2$,

if $\tau \leq \frac{\sqrt{\left(\frac{2}{(1+2\theta_s \mu)\theta_s} + \theta_s \Delta \right)^2 + \frac{4(\sigma-1)}{(1+2\theta_s \mu)} - \left(\frac{2}{(1+2\theta_s \mu)\theta_s} + \theta_s \Delta \right)}}{2}$, then $\xi \leq 0$. Suppose the above constraint holds, we have

$$\sum_{t=0}^{m-1} \mathbf{E} P(x_{t+1}^s) \leq \sum_{t=0}^{m-1} \mathbf{E} [(1-\theta_s)P(\tilde{x}^{s-1}) + \theta_s P(x^*) + \frac{\theta_s}{2\eta_s} (\|x^* - y_t^s\|^2 - \|x^* - y_{t+1}^s\|^2) + \theta_s^3 \mu L D + \frac{\theta_s^3 L D \Delta}{4\tau} + \frac{\theta_s^4 L D \Delta \mu}{\tau}]. \quad (42)$$

Using $\tilde{x}^s = \frac{1}{m} \sum_{t=0}^{m-1} x_{t+1}^s$, we obtain

$$\mathbf{E}[P(\tilde{x}^s) - P(x^*)] \leq \mathbf{E}[(1-\theta_s)(P(\tilde{x}^{s-1}) - P(x^*)) + \frac{\sigma L \theta_s^2}{2m} (\|y_0^s - x^*\|^2 - \|y_m^s - x^*\|^2) + \theta_s^3 \mu L D + \frac{\theta_s^3 L D \Delta}{4\tau} + \frac{\theta_s^4 L D \Delta \mu}{\tau}]. \quad (43)$$

Dividing both sides of (43) by θ_s^2 , summing over $s = 1$ to S , and using the definition $y_0^s = y_m^{s-1}$ and that $\frac{1-\theta_s}{\theta_s^2} \leq \frac{1}{\theta_{s-1}^2}$ when $\theta_s = \frac{2}{s+2}$, we have

$$\mathbf{E}[P(\tilde{x}^S) - P(x^*)] \leq \frac{4[P(\tilde{x}^0) - P(x^*)]}{(S+2)^2} + \frac{2\sigma L \|\tilde{x}^0 - x^*\|^2}{m(S+2)^2} + \frac{8(\Delta(1+\mu)/\tau + \mu)L D \log(S+2)}{(S+2)^2}. \quad (44)$$

□